Second International Conference on CFD in the Minerals and Process Industries
CSIRO, Melbourne, Australia
6-8 December 1999

THE FLOW IN CONICAL CYCLONES

J.Q. ZHAO and J. ABRAHAMSON

Department of Chemical and Process Engineering, Canterbury University, New Zealand

ABSTRACT

A CFD simulation of the fluid behaviour within a cyclone was carried out with FLUENT, using a nonsymmetric algebraic stress model. Some fluid features such as vortex-finder short cut flow and fall-off of axial and radial velocities with axial distance are noted. An analytical model was then developed for the separation region of the cyclone which could take the entry velocities as input. An exact solution of the equation of motion for steady axisymmetric inviscid flow in the conical region of a cyclone is given. The solution can represent the effects of potential flow, and non-uniform circulation, non-uniform total pressure received from the inlet region, on separation region streamline patterns.

Both a slot entry and an axial entry cyclone are examined. The velocity profiles predicted by FLUENT are compared with those of the analytical solution and with experimental measurements, for a number of axial locations. Reasonable agreement is found.

Using the analytical solution, the general effect of upstream vorticity from non-uniform circulation is discussed.

NOMENCLATURE

a_0 polynomial coefficients of 'circulation term'

A_i series expansion coefficient of Ψ_3^*

b_0 polynomial coefficients of 'total pressure'

B_i series expansion coefficient of Ψ_3^*

c_i arbitrary constant

H dimensionless total pressure

P dimensionless static pressure

R dimensionless conical radius, no. of r_w

r_w wall radius (from axis) at inlet boundary

R_c dimensionless cylindrical radius

v_i ith eigenvalue

$v_{\max u}$ maximum velocity at inlet boundary

V dimensionless fluid velocity, no. of $v_{\max u}$

V_r dimensionless fluid radial velocity (cylindrical radius)

V_x dimensionless fluid axial velocity

V_{xu} dimensionless fluid axial velocity at upstream boundary

V_φ dimensionless tangential fluid velocity (in longitude direction φ)

$V_{\varphi u}$ dimensionless fluid tangential velocity at upstream boundary

$Z_i(\theta)$ ith eigenfunction

Greek letters

α half angle of conical wall

Γ dimensionless circulation

θ colatitude

Ψ dimensionless streamfunction, $\psi / v_{\max u} r_w^2$

Ψ_1^* a part of the solution of this problem

Ψ_2^* a part of the solution of this problem

Ψ_3^* a part of the solution of this problem

INTRODUCTION

Cyclones can be used to separate almost any phase from another phase, and sometimes to classify particulates. Design normally involves estimation of the flow-field from inlet and other boundary conditions, with these conditions accepted as for a standard geometry, or systematically altered to attempt to find an improved performance. The difficulty here is the large number of possibilities with at least eight dimensions to consider, and a lack of confidence that the patchwork of assumptions will accurately predict trends.

CFD has been used with improving confidence (Pericleous, 1987; Davidson, 1988a; Hargreaves and Silvester, 1990; Hsieh and Rajamani, 1991; Dyakowski and Williams, 1993), but the time for optimization can become uneconomic. Analytical studies are still needed, which provide overall solutions quickly, with easier generation of design concepts (Bloor and Ingham, 1987; Davidson, 1988b). A combination of an analytical approach, alongside CFD studies, may be of more benefit.

In this paper we simulate the fluid behaviour within a return-flow cyclone with FLUENT. Then we give the overall features of the flowfields defined by the same inlet conditions, from analytical solutions of the simplified motion equations.

ANALYSIS

We use spherical polar co-ordinates (r, θ, φ) with corresponding velocity components $(v_r, v_\theta, v_\varphi)$. The origin is at the apex of the cone, the axis is along θ=0 and the surface of the cone boundary is on θ=α. If we introduce the streamfunction ψ, the motion for steady axisymmetric inviscid flow of an incompressible fluid can be described by the vorticity equation (Batchelor 1967, Bloor and Ingham 1987),

$$\frac{\partial^2\psi}{\partial r^2}+\frac{\sin\theta}{r^2}\frac{\partial}{\partial\theta}\left(\frac{1}{\sin\theta}\frac{\partial\psi}{\partial\theta}\right)=-\gamma\frac{d\gamma}{d\psi}+r^2\sin^2\theta\frac{dh}{d\psi} \quad \textbf{[1]}$$

$$v_r=\frac{1}{r^2\sin\theta}\frac{\partial\psi}{\partial\theta}$$

$$v_\theta=-\frac{1}{r\sin\theta}\frac{\partial\psi}{\partial r}$$

$\gamma = rv_\varphi \sin\theta$ is ($(2\pi)^{-1}$ times) the circulation round any axisymmetrically placed circle, and $h=\frac{p}{\rho}+\frac{1}{2}(v_\theta^2+v_r^2+v_\varphi^2)$ is (ρ^{-1} times) the total pressure. Both γ and h are functions of ψ alone.

We now introduce non-dimensional variables and also write the two terms on the right hand side of equation (1) in polynomial form. Since the dimensionless streamfunction can be defined so that it is always less than 1, higher order terms of this streamfunction may be ignored. A dimensionless form of equation (1) retaining only the first order terms, is

$$\frac{\partial^2\Psi}{\partial R^2}+\frac{\sin\theta}{R^2}\frac{\partial}{\partial\theta}\left(\frac{1}{\sin\theta}\frac{\partial\Psi}{\partial\theta}\right)=a_0+b_0R^2\sin^2\theta \quad \textbf{[2]}$$

Equation (2) can be used to describe many flow cases. Case I below can be used for a slot entry cyclone, and case II for axial entry.

Case I: Bloor and Ingham (1987) gave this example. Though they describe the flow field in spherical polar co-ordinates, they determine the upstream relationships in a *cylindrical* section. It was assumed that the flow is axially symmetric, and enters this region of the cyclone with a 'top hat' profile in the tangential velocity component $V_{\varphi u}$, and uniform (inward to the region) axial velocity V_{xu}. The radial velocity was chosen to ensure that it is zero at the cylindrical wall and that H is a constant. These upstream conditions are

$$\Psi=\frac{1}{2}V_{xu}\left(R_0^2-\frac{\Gamma^2}{V_{\varphi u}^2}\right),$$

$$H=\frac{1}{2}(V_{xu}^2+V_{\varphi u}^2+V_{ru}^2)+P=\text{constant}$$

where V_{ru} is the cylindrical radial velocity.

Equation (1) can then be simplified to

$$\frac{\partial^2\Psi}{\partial R^2}+\frac{\sin\theta}{R^2}\frac{\partial}{\partial\theta}\left(\frac{1}{\sin\theta}\frac{\partial\Psi}{\partial\theta}\right)=-\frac{V_{u\varphi}^2}{V_{xu}}=\text{constant}$$

This is a special case of equation (2), in which $a_0=-\frac{V_{\varphi u}^2}{V_{xu}}$, $b_0=0$.

Case II: This case is concerned with the constant b_0. The entering (dimensionless) circulation **Γ** is constant at a value Γ_u, the radial velocity at the upper boundary $V_r=0$, and the axial velocity there has a radial distribution $V_{xu}=c_1R_c^{\,2}+c_2$, (c_1, c_2 are arbitrary constants).

Since **Γ** is constant, the first part on the right of equation (1) is zero. Having assumed at entry the cylindrical radial velocity $V_r=0$, the radial equation of motion reduces here (for a steady flow) to

$$\frac{dP}{dR_c}=\frac{V_\varphi^2}{R_c}=\frac{\Gamma_u^{\,2}}{R_c^{\,3}}$$

Integrating the above equation $P=-\frac{\Gamma_u^{\,2}}{2R_c^{\,2}}+c_3$

(c_3 is an arbitrary constant)

so that

$$H=\frac{1}{2}(V_x^2+V_r^2+V_\varphi^2)+P$$

$$=\frac{1}{2}\left(V_{xu}^2+0+\frac{\Gamma_u^{\,2}}{R_c^{\,2}}\right)-\frac{\Gamma_u^{\,2}}{2R_c^{\,2}}+c_3=\frac{1}{2}V_{xu}^2+c_3 \quad \textbf{[3]}$$

The streamfunction at the upstream boundary can be calculated from

$$\Psi=\int R_cV_{xu}dR_c=\int R_c(c_1R_c^{\,2}+c_2)dR_c$$

$$=\frac{c_1R_c^{\,4}}{4}+\frac{c_2R_c^{\,2}}{2}+c_4=\frac{V_{xu}^2}{4c_1}+c_4-\frac{c_2^2}{4c_1}$$

(c_4 is an arbitrary constant) **[4]**

Combining (3) and (4), the relationship between streamfunction and the total pressure at the upstream boundary becomes

$$\Psi=\frac{H}{2c_1}+\text{constant}$$

Since the relationship will stay valid over the whole flowfield, $\frac{dH}{d\Psi}=2c_1$ over the flow field, and the equation (1) can be rewritten as

$$\frac{\partial^2\Psi}{\partial R^2}+\frac{\sin\theta}{R^2}\frac{\partial}{\partial\theta}\left(\frac{1}{\sin\theta}\frac{\partial\Psi}{\partial\theta}\right)=2c_1R^2\sin^2\theta$$

This is another special case to be described by equation (2), with $a_0 = 0$, $b_0 = 2c_1$.

A 'flexible solution' for equation (2) in a conical domain involving both a_0 and b_0 is:

$$\Psi = \Psi_1^* + \Psi_2^* + \Psi_3^* \qquad [5]$$

$$\Psi_1^* = \sum_{i=1}^{\infty} \frac{a_0 C_{ai} R^2}{(-\nu_i + 2)(\nu_i + 1)} Z_i(\theta)$$

$$\Psi_2^* = \sum_{i=1}^{\infty} \frac{b_0 C_{bi} R^4}{(-\nu_i + 4)(\nu_i + 3)} Z_i(\theta)$$

$$\Psi_3^* = \sum_{i=1}^{\infty} (A_i R^{-\nu_i + 1} + B_i R^{\nu_i}) Z_i(\theta)$$

The detail of eigenfunctions $Z_i(\theta)$ can be found in the appendix.

$$C_{ai} = \frac{\int_0^{\alpha} \frac{Z_i(\theta) d\theta}{\sin\theta}}{\int_0^{\alpha} \frac{Z_i^2(\theta) d\theta}{\sin\theta}}$$

$$C_{bi} = \frac{\int_0^{\alpha} Z_i(\theta) \sin\theta d\theta}{\int_0^{\alpha} \frac{Z_i^2(\theta) d\theta}{\sin\theta}}$$

SIMULATIONS

The simulations were carried out with FLUENT 3.03, using 3-dimensional nonsymmetric flow, and an algebraic stress model in polar coordinates. The conical wall was approximated by wall steps. The cyclone configuration for example I (Stairmand High Efficiency 1951) is presented in Fig. 1, and features a conventional cylinder-on-cone design with a single tangential inlet and an axial outlet. For example II, an axial (vane-like) inlet was taken.

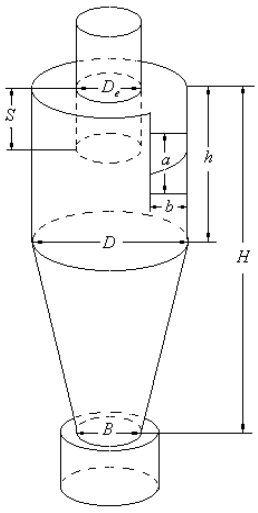

Figure1: Cyclone geometry (with De=1, D=2, H=8, h=3, a=1, b=0.40, S=1, B=0.75)

Example I Slot entry: Boundary conditions used were a flat tangential velocity profile across the inlet (22 m/s) and a fixed static pressure across the outlet section level with the roof.

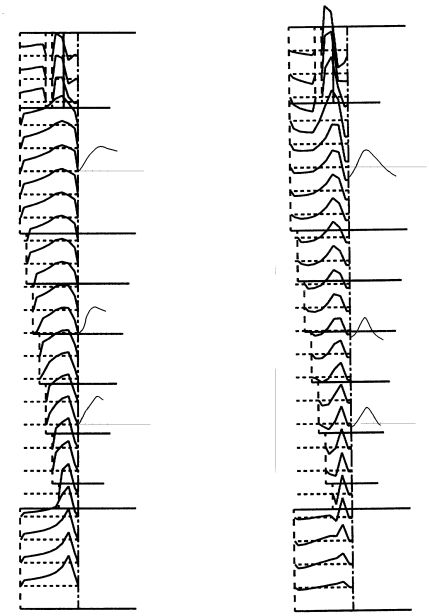

a. Tangential **b. Axial**

Figure 2: CFD (ASM) and measured velocity profiles for example I

Figs. 2a and Fig. 2b show the predicted tangential and axial velocity profiles respectively on the left sides. It is noted that there is a short cut flow under the vortex-finder, which passes through the upper portion of the cyclone and then flows into the vortex finder. We will discuss the short cut flow later. A central isolated core can also be noted, which is a region along the axis where the axial gas flow is in the reverse direction to the outflow. This air core is obvious when it occurs in hydrocyclones, but detailed measurements close to the core (Smith, 1962; Wakelin, 1993) show that a similar isolated region may also appear in gas cyclones.

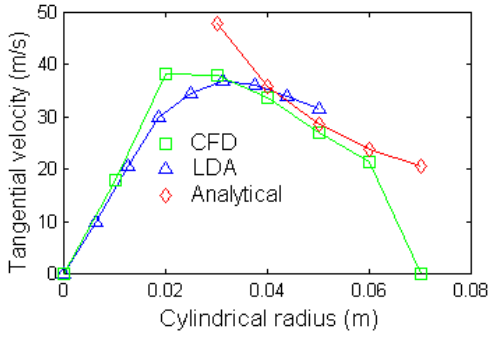

Figure 3a: Tangential velocity at middle position for example I (CFD is ASM model)

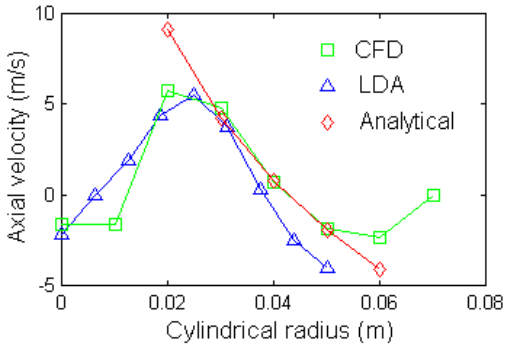

Figure 3b: Axial velocities at middle position for example I (CFD is ASM model)

Comparison with measured results (Boysan et al., 1983) is shown on the right sides in Figs. 2a and 2b with reasonable agreement at three heights. In Figs. 3a and 3b, the comparison at the middle position is shown in more detail, and a comparison with analytical solution is added.

Example II Axial entry

Boundary conditions were (1) a constant angular momentum for all entering fluid; (2) the radial velocity at the roof $V_r = 0$, and (3) the axial velocity there has a radial distribution $V_{xu} = c_1 R_c^{\,2} + c_2$, ($c_1$, c_2 are arbitrary constants).

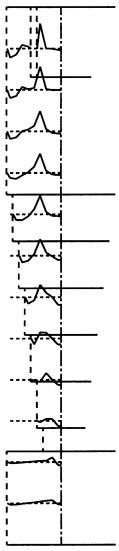

Figure 4: CFD (ASM) axial velocity profiles for example II

Fig.4 shows the CFD axial velocity profiles at different heights for this example. Comparing Figs. 4 and 2b, we find that the axial velocity in the conical portion of example II decreases faster towards the bin than in example I.

DISCUSSION

Since we used an early version of FLUENT to simulate the examples, the accuracy was restricted by some limitations. The number of cells was limited to 6001, with 20 steps around the perimeter, and 25 steps axially. Axial steps in the conical wall produced some artificial recirculation at the wall. Both $k-\varepsilon$ and ASM turbulence models were used. The normal $k-\varepsilon$ model hugely accentuated the core region compared with experiments, with the ASM model performing better in this respect. Experiments (Smith, 1962) show that the inflow boundary distribution of velocities and Reynolds stresses influence the velocity field. The $k-\varepsilon$ model showed more sensitivity to these upstream boundary conditions than did ASM.

When we simulated the flowfield of example I with CFD, we used boundary conditions very similar to those assumed for case I for the analytical solution, for which the solution is $\Psi_1^* + \Psi_3^*$. The comparisons in Fig.3 match over most of the separation working volume. Both analytical and CFD menthods can describe features of the flowfields, such as short cut flow, the fall-off of axial velocities along the axis, and a central isolated region (this can be modelled using the analytical method, but has not been shown here).

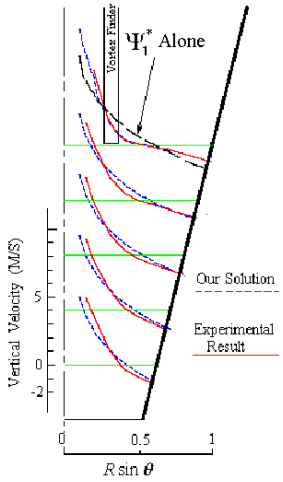

Figure 5: Comparison of the anlytical axial velocities with experimental findings of Kelsall's hydrocyclone ($\alpha = 10$ degrees) (<0.7% underflow, with air core)

Fig. 5 shows the comparison of the axial velocity of the analytical results of equation (2) with the corresponding experimental findings of Kelsall (1952. It can be seen that good agreement is obtained. Many experiments show that the flowfield just below the vortex finder may change acutely, and recirculating or shortcut flow may occur in this region. Our analytical solutions can quite accurately represent the flowfield in this region. The difference between our full solution and

Ψ_1^* for Kelsall's hydrocyclone comes mainly from the term Ψ_3^* of equation (5). Ψ_3^* is the solution where a_0 and b_0 are both zero, ie. for potential flow.

Any form of the distribution of axial velocity at the upper boundary can be matched using Ψ_3^*. However this term has its effect only on the upper and bottom portions of the cyclone, whereas in the main portion, the flowfield will revert automatically to that when this term is omitted. Smith (Smith 1962) has observed such similarity among flow patterns in a cylindrical cyclone, away from the entrance for varying inlet geometries and flows. The "adjusting fluid" corresponding to Ψ_3^* will pass through the upper portion of the cyclone and then flow into the vortex finder. This describes a shortcut flow. The shortcut flow is one of the factors decreasing the separating efficiency, since particles travelling with the fluid have had little time to separate.

Away from the upper boundary, the streamline pattern from equation (5) is given by the terms Ψ_1^* and Ψ_2^*.

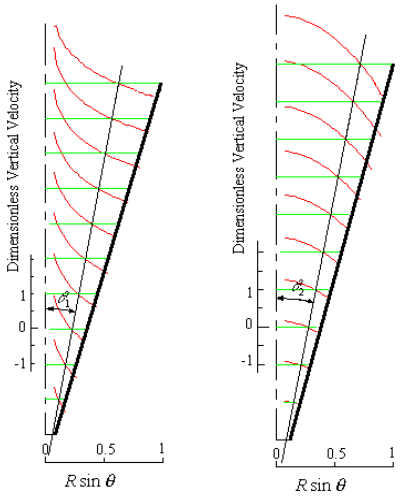

a, First Term Ψ_1^* b, Second Term Ψ_2^*

Figure 6 Axial Velocity Analytical

The first term Ψ_1^* of equation (5) represents the streamfunction caused by uneven distribution of *circulation* across the streamlines. The second term Ψ_2^* of equation (5) represents the streamfunction caused by uneven distribution of *total pressure* across the streamlines. Both these distributions introduce vorticity into the flowfield and make the fluid element rotate, so it can flow deeper into the cyclone. Fig. 6 a, b shows the axial velocity of Ψ_1^* and Ψ_2^* flow respectively. It can be seen that Ψ_2^* flows out in shorter paths, because it declines in R^4 order along the spherical radius R towards the vertex, while Ψ_1^* declines in R^2 order. The corresponding radial velocities (Fig. 7) reflect this axial dependence. They show for Ψ_1^*, constant values for a given angle θ from the axis, whereas for Ψ_2^*, values reduce in R^2 order. This is an important difference for particle collection.

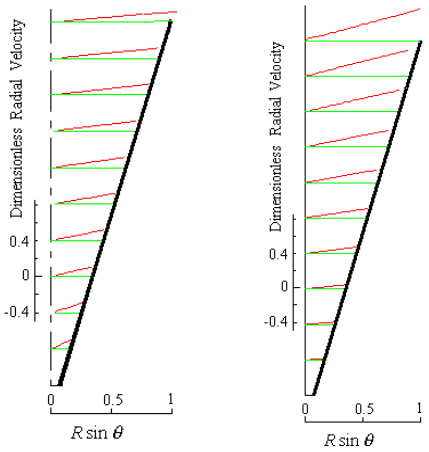

a, First Term Ψ_1^* b, Second Term Ψ_2^*

Figure 7: Radial Velocity Analytical

For many conventional slot entry cyclones, the boundary conditions for example I should be suitable, and the flow patterns will be similar to those of example I. We are unsure whether all axial entry cyclones are represented by example II.

In the design of cyclones, the 'natural length' of the vortex in cyclones is an important concept. It can be argued that 'natural length' is related to the penetration of the above flows and thus to upstream boundary conditions. From the argument above, a tentative conclusion is that the natural length of a given cyclone body will be less with an axial entry than with a slot entry.

CONCLUSIONS

1. A CFD simulation of a conical cyclone with FLUENT 3.03 was carried out. The results are rough but suitable for comparison.
2. An exact solution of the equation of motion for steady axisymmetric inviscid flow in the conical region of a cyclone is found. The solution can be used to describe the flowfield of practical cyclones.
3. The upstream boundary conditions at the entrance have a key effect on the flow pattern of cyclones.
4. The effect can be described by the upstream vorticity distributions, which are formed from the inlet structure and boundary layer.

REFERENCES

BATCHELOR, G. K. (1967) *An introduction to Fluid dynamics*. Cambridge University Press, London. 543-555.

BLOOR, M. I. G. and INGHAM, D.B., (1987), "The flow in industrial cyclones", *Journal of Fluid Mechanics* **178**, 507-519.

BOYSAN, F. and et al, (1983), "Experimental and theoretical studies of cyclone separator aerodynamics", *Proc. I. Chem. E. Symposium series* no.**69,** 305-317.

BOYSAN, F, and et al, (1986), "Mathematical Modelling of Gas-Particle Flows in Cyclone Separator", *Encyclopedia of Fluid Mechanics*, **4**, N.P. Cheremisionoff, Ed., Gulf Publ. Co., Book Division, Houston TX, 1307-1329.

DAVIDSON, M. R., (1988a), "Numerical calculations of flow in a hydrocyclone operating without an air core", *Appl. Math. Modelling,* **12**,119-128.

DAVIDSON, M. R., (1988b), "Similarity solutions for flow in hydrocyclones", *Chem Eng Sci,***43,** 1499-1505.

DYAKOWSKI, T. and WILLIAMS, R.A., (1993), "Modelling turbulent flow within a small-diameter hydrocyclone" , *Chem Eng Sci,* **48**, 1143-1152.

HARGREAVES, J. H. and SILVESTER, R. S. (1990), "Computational fluid dynamics applied to the analysis of deoiling hydro-cyclone performance", *Trans I Chem E,* **68,** part A, 365-383.

HSIEH, K. T. and RAJAMANI, R. K., (1991), "Mathematical model of the hydrocyclone based on physics of fluid flow", *AIChE J,* **37,** 735-746.

KELSALL, D.F., (1952), "A study of the motion of solid particles in a hydraulic cyclone", *Trans. I. Chem. E.* **30**, 87-108.

PERICLEOUS, K.A., (1987), "Mathematical simulation of hydrocyclones", *Appl. Math. Modelling,***11,** 242-255.

SMITH, J.L., (1962), "An experimental study of the vortex in the cyclone separator", *J. Basic Eng. Trans. A.S.M.E.* **84D**, 602-608.

STAIRMAND, C. J. (1951), "The design and performance of cyclone separators", *Trans. I.. Chem. E.,* **29,** 356-383.

APPENDIX: Details of functions $Z_i(\theta)$

$$Z_i(\theta) = p_i^*(\theta) - \frac{p_i^*(0)}{q_i^*(0)} q_i^*(\theta)$$

$$p_i^*(\theta) = \frac{(\nu_i - 1)\int_0^\theta \cos^{\nu_i - 2}(\theta) p_i(\cos\theta) d(\cos(\theta))}{\cos^{\nu_i - 1}(\theta)}$$

$p_i(\cos\theta)$ is the first kind of Legendre function

$$q_i^*(\theta) = \frac{(\nu_i - 1)\int_0^\theta \cos^{\nu_i - 2}(\theta) q_i(\cos\theta) d(\cos(\theta))}{\cos^{\nu_i - 1}(\theta)}$$

$q_i(\cos\theta)$ is the second kind of Legendre function

ν_i is the eigenvalue of equation

$$Z_i(\alpha) = p_i^*(\alpha) - \frac{p_i^*(0)}{q_i^*(0)} q_i^*(\alpha)$$

$$A_i = \frac{R_s^{\nu_i}\left(\int_0^\alpha \frac{10\Psi(R_e,\theta)Z_i(\theta)d\theta}{\sin\theta} + a_0 R_e^2 Z_{1ig} - b_0 R_e^4 Z_{2ig}\right) - R_e^{\nu_i}\left(\int_0^\alpha \frac{10\Psi(R_s,\theta)Z_i(\theta)d\theta}{\sin\theta}\right.}{Z_{ig}(R_e^{-\nu_i+1}R_s^{\nu_i} - R_e^{\nu_i}R_s^{-\nu_i+1})}$$

$$\frac{\left. + a_0 R_s^2 Z_{1ig} - b_0 R_s^4 Z_{2ig}\right) + ((\Psi(R,\alpha) - \Psi(R,0))Z_{3ig} + \Psi(R,0)Z_{4ig})(R_s^{\nu_i} - R_e^{\nu_i})}{}$$

$$B_i = \frac{R_s^{-\nu_i+1}\left(\int_0^\alpha \frac{10\Psi(R_e,\theta)Z_i(\theta)d\theta}{\sin\theta} + a_0 R_e^2 Z_{1ig} - b_0 R_e^4 Z_{2ig}\right) - R_e^{-\nu_i+1}\left(\int_0^\alpha \frac{10\Psi(R_s,\theta)Z_i(\theta)d\theta}{\sin\theta}\right.}{Z_{ig}(R_e^{\nu_i}R_s^{-\nu_i+1} - R_e^{-\nu_i+1}R_s^{\nu_i})}$$

$$\frac{\left. + a_0 R_s^2 Z_{1ig} - b_0 R_s^4 Z_{2ig}\right) + ((\Psi(R,\alpha) - \Psi(R,0))Z_{3ig} + \Psi(R,0)Z_{4ig})(R_s^{-\nu_i+1} - R_e^{-\nu_i+1})}{}$$

$$Z_{ig} = 10\int_0^\alpha \frac{Z_i^2(\theta)d\theta}{\sin\theta}$$

$$Z_{1ig} = \int_0^\alpha 5(C_\alpha - \ln(0.5\tan\theta) - \frac{1}{1+\cos\theta})(\sin\theta)Z_i(\theta)d\theta$$

with

$$C_\alpha = \cos ec^2\alpha + \ln(0.5\tan\alpha) - \cos ec\alpha\cot\alpha$$

$$Z_{2ig} = \int_0^\alpha (1 - \frac{1-5\cos^2\theta}{1-5\cos^2\theta})(\sin\theta)Z_i(\theta)d\theta$$

$$Z_{3ig} = \int_0^\alpha \frac{-10}{(1+\cos\theta)(1-\cos\alpha)}(\sin\theta)Z_i(\theta)d\theta$$

$$Z_{4ig} = \int_0^\alpha \frac{-10}{\sin\theta} Z_i(\theta)d\theta$$

These functions can be readily calculated using a number of commercial packages, eg. Matlab.